2021 IEEE 4th International Conference on Soft Robotics (RoboSoft)
April 12-16, 2021, Yale University, USA

Design Parameters for Stacked-Ribbon Shape-Memory Alloy Bending Actuators*

Trevor L. Buckner, Rebecca Kramer-Bottiglio

2021 IEEE 4th International Conference on Soft Robotics (RoboSoft) | 978-1-7281-7713-7/20/$31.00 ©2021 IEEE | DOI: 10.1109/RoboSoft51838.2021.9479427

***Abstract*— Soft robots continue to suffer from a lack of powerful actuator options that do not rely upon bulky external power supplies or fluid pumps. This is especially true of bending-type actuators that often require immersion in an ionic or aqueous fluid, or fail to provide adequate forces for more than trivial tasks. Shape memory alloys (SMA) have recently seen use as a bending actuator that occupies little space, provides large forces, and can be powered from a small on-board battery. In this work, we investigate design parameters of bending SMA actuators made from flattened Nitinol wires—referred to as SMA ribbons—which possess a geometry favorable to repeatable bending actuation. We then present a novel "stacked" SMA ribbon actuator that provides increased bending forces while reducing overall system stiffness, compared to a single thick SMA ribbon.**

I. Introduction

In addition to flexible components, soft robots often require parts that are small, lightweight, and self-contained. In the case of actuators, a large percentage of soft robots utilize vacuum or pressure-based systems, requiring a heavy external pump or fluidic storage to which the robot remains tethered. In the move toward untethered operation[1], there have been numerous approaches toward the concept of "artificial muscles"[2], generally implying a thin, possibly fiber-like form factor that can provide motion intrinsically, rather than via external volume displacement from a pump or an off-camera cable drive. Normally, these artificial muscles exhibit strictly contractile or extensile motions, as in the cases of super-coiled nylon muscles[3], conductive polymers such as polypyrrole[4], dielectric Peano-HASEL actuators[5], shape memory polymers[6], shape memory alloy springs[7], or electromechanical spun carbon nanotubes[8]. On the other hand, some pure-bending actuators have also been developed, including electroactive polymer composites[9] and hydrogels[10], although both of these tend to suffer from extremely slow actuation times and low forces. Recently, research has begun to utilize Shape Memory Alloys (SMA) in flattened sheets or ribbons as an electrically-controlled bending actuator, which provides higher output forces and displacements in applications where the profile of the robot must remain extremely thin [11]–[13]. Herein, we offer characterizations of a Nitinol SMA bending ribbon actuator, and its performance as influenced by programming shape and cross-sectional geometry. We further introduce a novel "stacked" SMA ribbon actuator that offers greater net force for antagonistic actuation while also reducing overall system rigidity for soft applications.

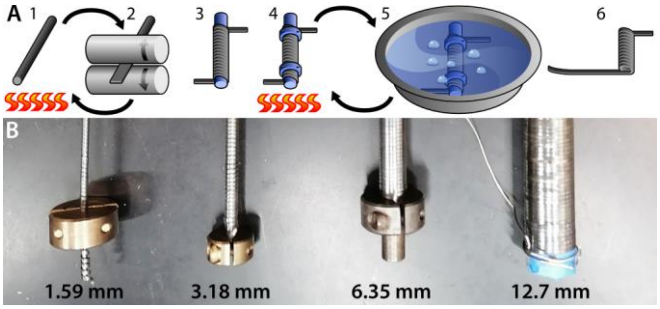

Figure 1. SMA ribbon actuator manufacture. (**A**) SMA wire is softened via annealing (1) and then flattened in a rolling mill (2), repeating these steps until desired thickness is reached; the flattened ribbon is wrapped around a steel rod (3), and clamped in place (4); the rod is heated and quenched (5), repeated three times; the ribbon is removed from the rod and unwrapped (6). (**B**) SMA ribbons prepared for programming by wrapping around steel rods of varying diameter and clamping in place.

II. Materials And Methods

A. Preparing SMA Ribbons

Shape Memory Alloy ribbons are formed from round Nitinol wire (Memry), with the initial wire diameter selected depending on the desired cross-section of the resulting ribbon. Building from the process first described in [13], the round wire is first softened by annealing in an oven for 20 minutes at 500 °C. After air-cooling, the softened wire is passed through a simple manual rolling mill machine, reducing the thickness in incremental steps of approximately 10 μm. Ribbons are annealed between steps as needed to relieve any work hardening and prevent damage to the equipment. Note that the total cross-sectional area is reduced somewhat as the ribbon is elongated during this process.

In this work, specimens are flattened into two sizes: 410 × 1,070 μm from the initial round diameter of 762 μm (0.03 in), and 140 × 1,070 μm from an initial round diameter of 508 μm (0.02 in), hereafter referred to as "thick" and "thin" ribbons. Note that the total cross-sectional area of the thin ribbon is almost exactly 1/3 that of the thick ribbon.

B. Programming SMA Ribbons for Bending Motion

Prepared SMA ribbons are tightly wrapped, flush around a 316 stainless steel rod and clamped in place via a split-shaft collars (McMaster-Carr) at both ends of the wrapped coil. The rod is then placed in an oven at 390 °C for 20 minutes, after which the rod is removed and quickly quenched in room-temperature water for 30 seconds until fully cooled. This heating and quenching step is repeated three times. Then, the SMA ribbon is unclamped and straightened, ready to actuate back into a curled configuration (Fig. 1A). All specimens in this work were programmed in the same batch.

* Research supported by NASA.

R. Kramer-Bottiglio is with the School of Engineering and Applied Science, Yale University of New Haven, Connecticut, CT 06520 USA, (phone: 203-432-9662; e-mail: rebecca.kramer@yale.edu).

T. L. Buckner is with the School of Engineering and Applied Science, Yale University of New Haven, Connecticut, CT 06520 USA, (e-mail: trevor.buckner@yale.edu).

III. Results

Flattening an SMA wire into a thin ribbon provides a geometry favorable to repeatable bending actuation. We have shown in a previous work that while a round wire may twist out of plane or roll around, thin ribbons with greater cross-sectional aspect ratios are able to more efficiently direct their forces along the programmed trajectory[13]. That is, a flat ribbon will provide larger bending forces than a round wire of similar area moment of inertia. In this work, we focus on further characterization of ribbon actuators.

A. Effect of Coil Programming Diameter

It is well-known that the performance of a contracting spring actuator made from SMA wire will vary greatly depending on the chosen coil diameter and pitch angle during the programming step[14]. However, the analogous properties for bending actuators are understudied. Here, we characterize the impact of programmed curvature by measuring the performance of a set of bending actuators, programmed by wrapping SMA ribbons about stainless steel rods of varying diameter: 1.59, 3.18, 6.35, and 12.7 mm (1/16, 1/8, 1/4, and 1/2 inches, Fig. 1B). In each case, unwrapping and then heating the ribbons to 100 °C under free deflection caused the actuator to return to its fully coiled state without any discernible loss to the overall stroke curvature.

Using a universal testing machine (Instron 3345) to perform a 3-point bending test with a support span of 3 mm, we measured the bending rigidity of the SMA ribbons, bending each specimen (5 per program diameter) opposite its normal actuation direction (Fig. 2A). The flexural rigidity (EI) becomes noticeably higher as the coils are wrapped more tightly, approximately following a power series curve with changing programmed diameter (Fig. 2B).

Similar specimens for each programmed diameter were also measured for blocked bending tip force generation using a Dynamic Mechanical Analyzer (TA Instruments, DMA Q850). Specimens were placed in a single-cantilever fixture with a constraining plate on one face to prevent the ribbon from popping up. The free end of the specimen was placed precisely on the force probe and then subjected to a temperature ramp from 20 °C to 120 °C at a rate of 3 °C/min (Fig. 2C). Interestingly, the smallest programming diameter appeared to cause a delay of about 10 °C in the onset of force generation. This delay may be a result of over-straining during the wrapping stage, resulting in small dislocations that inhibit the austenite-martensite transition that governs actuation until reaching a higher temperature[15]. It is important to note that for the particular alloy used, the safe activation temperature is 100 °C, and moving beyond that point for extended periods risks "burning out" the actuator by inadvertently annealing the material and reverting the programmed state. Knowing this, it is apparent that the actuators programmed at the tightest diameter (1.59 mm) are unable to fully activate within the safe temperature region (Fig. 2C), while the loosest diameter (12.7 mm) is unable to generate a large amount of force even beyond 120 °C, simply because its programmed bend angle is so shallow (Fig. 2D).

Observing the above results, it becomes clear that for the range of programmed diameters tested in this work, the 6.35 mm size has the highest ratio of output force to flexural

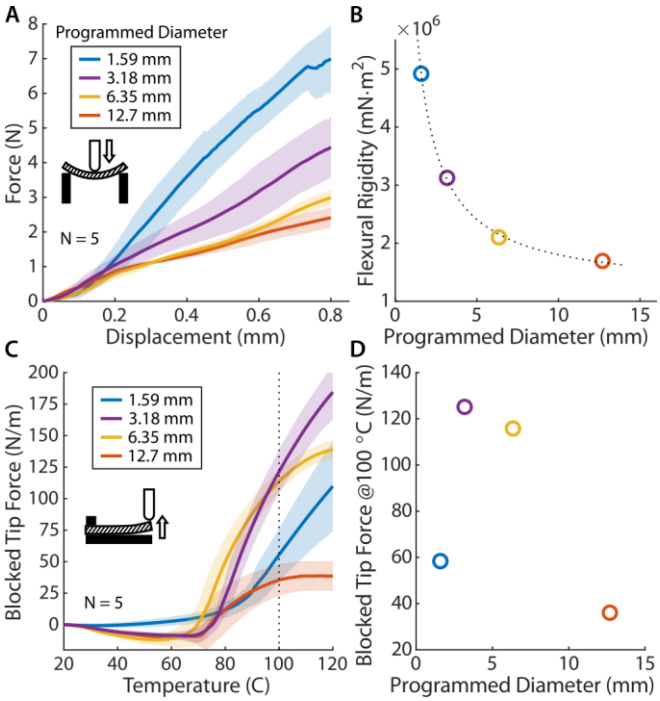

Figure 2. SMA bending actuator performance dependent on initial programmed diameter. (**A**) Force-displacement curve for specimens in a 3-point bending test, bent opposite the actuation direction. (**B**) Flexural rigidity calculated from (A). (**C**) Blocked bending tip force over a temperature ramp. 100 °C is the maximum safe operating temperature. (**D**) Mean blocked tip force at 100 °C.

rigidity, although we expect that the optimal point will vary depending on the particular alloy and specimen cross-section. This further suggests that SMA ribbons designed to perform more complex bending motions, such as moving into an alternating "ripple" pattern, or forming a radially-compressive "clover" could be optimized by programming each curve along the entire ribbon with a specified, and perhaps varying radius of curvature, to meet localized force and rigidity targets (Fig. 3A).

B. Stacked Actuator Performance

We developed a "stacked" SMA actuator, composed of several thin ribbons layered, but not adhered, on top of each other. This stacked configuration essentially multiplies the output force of the actuator while mitigating much of the rigidity that would be present in a single thicker ribbon, following classical beam theory. In evaluating this novel stacked SMA actuator, we performed the same tests again as described in Section A to characterize the effective flexural rigidity and the blocked tip force for each actuator configuration. In this case, we compared a single thin ribbon, a single thick ribbon (Fig. 3B), a stack of 3 thin ribbons ("3-stack", equivalent cross-sectional area as the thick ribbon), and a stack of 6 thin ribbons ("6-stack", Fig. 3C). Each of these configurations was programmed using the 6.35 mm diameter steel rods.

Observing the results, we note that the thick actuator has a drastically (19.4×) higher flexural rigidity than the thin actuator (Fig 3D, E), while only providing 3.2× the force (Fig. 3F, G). On the other hand, the 6-stack has a flexural rigidity of 4.6× the thin ribbon but provides 3.0× the force. Ideally, the 3- and 6-stack would provide 3- and 6× the force

of the thin actuator, respectively, but we suspect that performance is reduced due to interfacial losses between the many layers, and the tendency for the ribbons to slide apart if not bundled together with crimps or tightly wrapped thread.

Stacked SMA ribbon actuators may be useful for antagonistic actuation. Previous work has confirmed that bending SMA actuators are indeed capable of delivering the required forces to bend an opposing actuator, although doing so consumes energy, reducing the total force available for performing work toward a chosen task[13]. By using thinner wires in a stacked configuration, the ratio of flexural rigidity to actuation force can be decreased, resulting in higher net forces in an antagonistic setting (Fig. 3H). Given the force F at 100 °C, and flexural modulus K of two different SMA actuators, the formula $(F_{6\text{-stack}}/F_{thick})\cdot(K_{thick}/K_{6\text{-stack}})$ compares the rigidity/force ratio between two actuator types, and indicates that simply exchanging a thick actuator for a 6-stack would provide a 3.9× increase in the percentage of input force remaining as net force, while a 3-stack would provide an increase of 5.2×.

C. Stacked Actuator Cooling Time

A known bottleneck in SMA actuation is cooling time, which can require several seconds between actuation strokes[16], particularly because an SMA becomes 2-3 times more rigid when active[17], which prevents antagonistic motion until the opposing actuator has cooled. The cooling time can be severely impacted by proximity to insulating materials in the host robotic structure, as well as the volume and thickness of the SMA component. We investigated this characteristic for each of the different actuator configurations in free convection. Every specimen (5 of each) was lightly coated in a high-emissivity ink, and then suspended between two non-conducting supports. Specimens were then Joule-heated above 100 °C. The power was then disconnected, and the temperatures were recorded over time using a thermal camera (Fluke TiX 580). The thin actuators cooled to room temperature (22 °C) within 20 seconds, while both the 3-stack and thick actuators took approximately twice as long due to their increased mass (Fig. 3I). Interestingly, the increased surface-area-to-volume ratio of the 3-stack compared to the thick ribbon did not seem to provide any reduction in cooling time, which may have been a result of each layer in the stack being pressed tightly together, concealing the interfacial surfaces during the test.

IV. Conclusion

The technique of using SMA ribbons as a bending-type actuator is relatively young, but also holds significant promise for the field of soft robotics, among others. By intelligently selecting the design parameters of the ribbon, including thickness, programming angle, and even stacking of multiple ribbons, the net force and overall system rigidity can be tuned to better suit the desired application performance, including localized regions of increased or reduced forces. We expect that the stacked actuator design can be further improved by using greater numbers of thinner ribbons. Further, we suspect that by including a thin, conductive bonding layer between ribbons, such as a liquid-metal/elastomer composite[18], cooling time could be further reduced[19], taking advantage of the increased surface area for heat dissipation while keeping ribbons attached to each other in a way that still allows independent flexure.

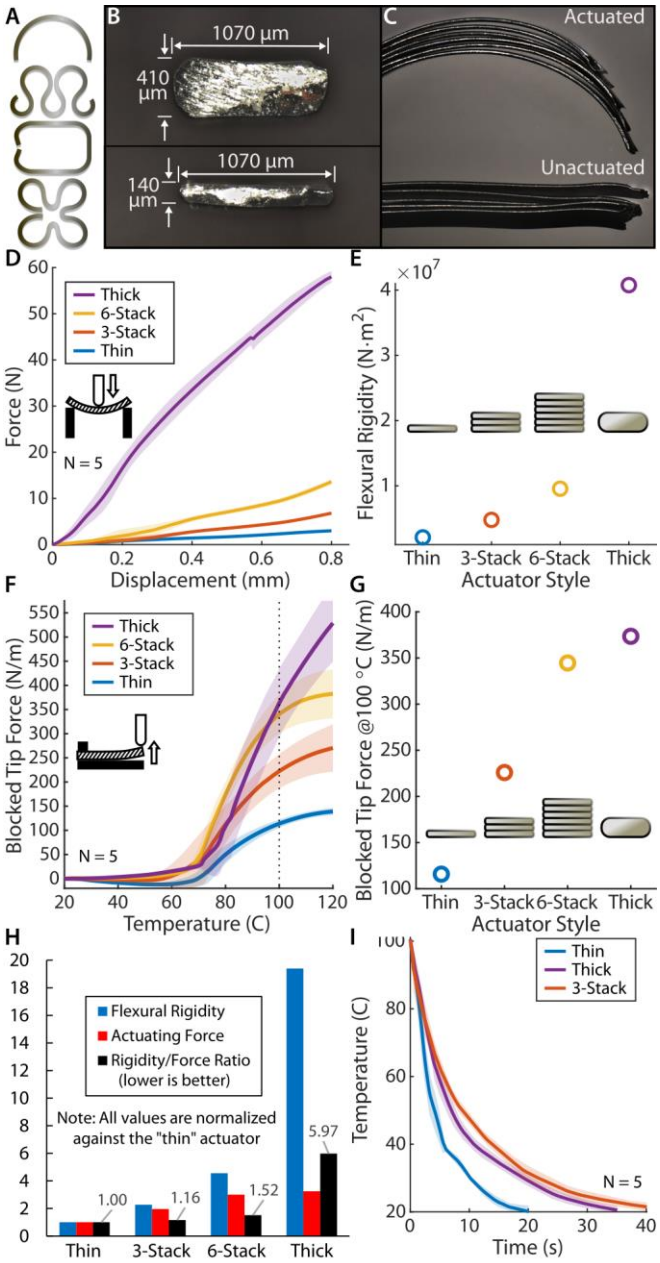

Figure 3. SMA bending actuator performance of thin, thick, 3-stack, and 6-stack configurations. (**A**) Example sketches of potential complex ribbons using varied programmed diameters, including a circular curve, a serpentine ripple, a right-angled polygon, and a compressive clover. (**B**) Microscope cross-sections of thin and thick ribbons. (**C**) 6-stack actuator in the actuated, curved position, and in the unactuated straight position. (**D**) Force-displacement curve for specimens in a 3-point bending test, bent opposite the actuation direction. (**E**) Flexural rigidity calculated from (D). (**F**) Blocked bending tip force over a temperature ramp. 100 °C is the maximum safe operating temperature. (**G**) Mean blocked tip force at 100 °C. (**H**) Relative performace of each actuator configuration, normalized against the "thin" ribbon. (**I**) The thin actuator takes approximately 20 s to cool to 22 °C, while the thick and 3-stack actuators take 35 and 40 s respectively.

Acknowledgment

This work was supported by The National Aeronautics and Space Administration (grant no. 80NSSC17K0553).

REFERENCES

[1] S. I. Rich, R. J. Wood, and C. Majidi, "Untethered soft robotics," *Nature Electronics*, vol. 1, no. 2, Art. no. 2, Feb. 2018, doi: 10.1038/s41928-018-0024-1.

[2] S. M. Mirvakili and I. W. Hunter, "Artificial Muscles: Mechanisms, Applications, and Challenges," *Adv. Mater.*, vol. 30, no. 6, p. 1704407, Feb. 2018, doi: 10.1002/adma.201704407.

[3] S. M. Mirvakili *et al.*, "Simple and strong: twisted silver painted nylon artificial muscle actuated by Joule heating," San Diego, California, USA, Mar. 2014, vol. 9056, p. 90560I, doi: 10.1117/12.2046411.

[4] J. Foroughi, G. M. Spinks, and G. G. Wallace, "High strain electromechanical actuators based on electrodeposited polypyrrole doped with di-(2-ethylhexyl)sulfosuccinate," *Sensors and Actuators B: Chemical*, vol. 155, no. 1, pp. 278–284, Jul. 2011, doi: 10.1016/j.snb.2010.12.035.

[5] N. Kellaris, V. G. Venkata, G. M. Smith, S. K. Mitchell, and C. Keplinger, "Peano-HASEL actuators: Muscle-mimetic, electrohydraulic transducers that linearly contract on activation," *Science Robotics*, vol. 3, no. 14, Jan. 2018, doi: 10.1126/scirobotics.aar3276.

[6] Y. Meng, J. Jiang, and M. Anthamatten, "Body temperature triggered shape-memory polymers with high elastic energy storage capacity," *J. Polym. Sci. Part B: Polym. Phys.*, vol. 54, no. 14, pp. 1397–1404, Jul. 2016, doi: 10.1002/polb.23990.

[7] S. Kim, E. Hawkes, K. Choy, M. Joldaz, J. Foleyz, and R. Wood, "Micro artificial muscle fiber using NiTi spring for soft robotics," in *2009 IEEE/RSJ International Conference on Intelligent Robots and Systems*, St. Louis, MO, USA, Oct. 2009, pp. 2228–2234, doi: 10.1109/IROS.2009.5354178.

[8] W. Guo *et al.*, "A Novel Electromechanical Actuation Mechanism of a Carbon Nanotube Fiber," *Adv. Mater.*, vol. 24, no. 39, pp. 5379–5384, Oct. 2012, doi: 10.1002/adma.201201845.

[9] A. Punning, M. Kruusmaa, and A. Aabloo, "A self-sensing ion conducting polymer metal composite (IPMC) actuator," *Sensors and Actuators A: Physical*, vol. 136, no. 2, pp. 656–664, May 2007, doi: 10.1016/j.sna.2006.12.008.

[10] Z. Han *et al.*, "Dual pH-Responsive Hydrogel Actuator for Lipophilic Drug Delivery," *ACS Appl. Mater. Interfaces*, vol. 12, no. 10, pp. 12010–12017, Mar. 2020, doi: 10.1021/acsami.9b21713.

[11] H. F. M. Ali, A. M. Khan, H. Baek, B. Shin, and Y. Kim, "Modeling and control of a finger-like mechanism using bending shape memory alloys," *Microsyst Technol*, Jan. 2021, doi: 10.1007/s00542-020-05166-0.

[12] J. K. Paik and R. J. Wood, "A bidirectional shape memory alloy folding actuator," *Smart Mater. Struct.*, vol. 21, no. 6, p. 065013, May 2012, doi: 10.1088/0964-1726/21/6/065013.

[13] T. L. Buckner, R. A. Bilodeau, S. Y. Kim, and R. Kramer-Bottiglio, "Roboticizing fabric by integrating functional fibers," *PNAS*, vol. 117, no. 41, pp. 25360–25369, Oct. 2020, doi: 10.1073/pnas.2006211117.

[14] J. Koh, "Design of Shape Memory Alloy Coil Spring Actuator for Improving Performance in Cyclic Actuation," *Materials*, vol. 11, no. 11, Art. no. 11, Nov. 2018, doi: 10.3390/ma11112324.

[15] E. Alarcon *et al.*, "Fatigue performance of superelastic NiTi near stress-induced martensitic transformation," *International Journal of Fatigue*, vol. 95, pp. 76–89, Feb. 2017, doi: 10.1016/j.ijfatigue.2016.10.005.

[16] Y. Tadesse, N. Thayer, and S. Priya, "Tailoring the Response Time of Shape Memory Alloy Wires through Active Cooling and Pre-stress," *Journal of Intelligent Material Systems and Structures*, vol. 21, no. 1, pp. 19–40, Jan. 2010, doi: 10.1177/1045389X09352814.

[17] K. Otsuka and C. M. Wayman, *Shape Memory Materials*. Cambridge University Press, 1999.

[18] S. Rich, S.-H. Jang, Y.-L. Park, and C. Majidi, "Liquid Metal-Conductive Thermoplastic Elastomer Integration for Low-Voltage Stiffness Tuning," *Advanced Materials Technologies*, vol. 2, no. 12, p. 1700179, Dec. 2017, doi: 10.1002/admt.201700179.

[19] M. Leary, F. Schiavone, and A. Subic, "Lagging for control of shape memory alloy actuator response time," *Materials & Design*, vol. 31, no. 4, pp. 2124–2128, Apr. 2010, doi: 10.1016/j.matdes.2009.10.010.